Sains Malaysiana 52(3)(2023): 981-992
http://doi.org/10.17576/jsm-2023-5203-21

Characteristics of Different Groups of Flare-CME in the Minimum to Rising Phase of Solar Cycle 24

(Pencirian Kumpulan Berbeza Suar-CME dalam Fasa Minimum hingga Fasa Menaik Kitaran Suria 24)

N. Mohamad Ansor[1,2], Z.S. Hamidi[1,2,*] & N.N.M. Shariff[2,3]

[1]School of Physics and Material Science, Faculty of Applied Sciences
Universiti Teknologi MARA, 40450 Shah Alam, Selangor Darul Ehsan, Malaysia
[2]Institute of Science, Universiti Teknologi MARA, 40450 Shah Alam, Selangor Darul Ehsan, Malaysia
[3]Academy Contemporary Islamic Studies, Universiti Teknologi MARA, 40450 Shah Alam, Darul Ehsan, Malaysia

Received: 17 July 2022/Accepted: 9 January 2023

ABSTRACT

Coronal Mass Ejections are significant solar events that involve intense explosions of magnetic fields and mass particles out from the corona. As the hot plasma are brought by the solar wind into the Earth's magnetosphere, geomagnetic storm is generated and causing malfunctions in telecommunication and power systems. This study is aimed to investigate the distribution of flare-CMEs characteristics which occurred at the beginning phase of solar cycle 24, from Dec. 2008 until Dec. 2013. In the analysis, all events are classified according to their class of flares associated with the CMEs. The CMEs that are accompanied by A, B, and C flares are categorized as low group flare-CME, while CMEs with M and X flares are placed under high group flare-CME. Afterwards, they are analyzed to observe the distribution of their main CME properties; velocity, acceleration and angular width. At the end of the study, we found that velocity and angular width are the two properties that have high influential for high and low groups, with R value of 0.36 and 0.67, respectively. Most of high group flare-CMEs showed up in 360° as well as low group flare-CMEs if the associated minor flares lasted longer than 30 min. Furthermore, the speed range of 360° high and low class flare-CME cannot be defined from the results since all of them propagated at fluctuating velocity. Hence, it is believed that full halo CMEs have no velocity boundary as they can travel from 500 km/s and go beyond 2500 km/s.

Keywords: CME properties; coronal mass ejections, solar cycle 24; solar flare

ABSTRAK

Lentingan Jisim Korona ialah peristiwa suria yang ketara yang melibatkan letupan kuat medan magnet dan zarah jisim keluar daripada korona. Apabila plasma panas dibawa oleh angin suria ke dalam magnetosfera Bumi, ribut geomagnet terhasil dan menyebabkan kerosakan dalam sistem telekomunikasi dan kuasa. Kajian ini bertujuan untuk mengkaji taburan ciri suar-CME yang berlaku pada fasa permulaan kitaran suria 24, dari Dis. 2008 hingga Dis. 2013. Dalam analisis ini, semua kejadian dikelaskan mengikut kelas suar mereka yang dikaitkan dengan CME. CME yang diikuti dengan suar A, B dan C dikategorikan sebagai kumpulan rendah suar-CME, manakala CME dengan suar M dan X diletakkan di bawah kumpulan tinggi suar-CME. Selepas itu, semua kejadian dianalisis untuk memerhatikan taburan sifat CME utama; halaju, pecutan dan lebar sudut. Pada akhir kajian, kami mendapati halaju dan lebar sudut adalah dua sifat yang mempunyai pengaruh tinggi untuk kumpulan tinggi dan rendah dengan nilai R masing-masing 0.36 dan 0.67. Kebanyakan suar-CME kelas tinggi muncul dalam 360° serta suar-CME kelas rendah jika suar kecil yang berkaitan berlangsung lebih lama daripada 30 minit. Tambahan pula, julat kelajuan 360° kumpulan tinggi dan rendah suar-CME tidak boleh ditakrifkan daripada keputusan kerana kesemuanya merambat pada halaju turun naik. Oleh itu, dipercayai bahawa CME halo penuh tidak mempunyai sempadan halaju kerana ia boleh bergerak dari 500 km/s dan melepasi 2500 km/s.

Kata kunci: Kitaran suria 24; lentingan jisim korona; sifat CME; suar suria

Introduction

A Coronal Mass Ejection (CME) is known as an enormous and powerful explosion of magnetic field and mass particles released from the Sun's corona. It was viewed as a substantial structure expelled from the Sun when firstly discovered in white-light observation (Tousey 1973). CMEs are theoretically recognized as the main factor in space weather (Gosling 1994) because their emergences can lead to geomagnetic disturbances which result in breakdown in many systems, including radio transmissions and satellites. CMEs take place in active regions and complex regions with filaments and prominences where enlarged closed magnetic loops extended to the solar surface. An earlier model demonstrated that the magnetic buoyancy contributed to the eruption of CMEs and their formations tended to go with falling materials with enormous masses (Wolfson et al. 1997). The following study in 2010 opposed several models that correlated the CMEs with explosion flare heating, as they discovered only small heating presence during the eruptions (Mittal et al. 2010).

Over a decade, the possibility of CMEs to be categorized in different classes have been on the lookout in many studies (Andrews et al. 2001). A very advance study in 1983 analyzed 12 events on their heigh-speed data and they proposed two different classes of CMEs from the results (MacQueen et al. 1983). All 12 CME events displayed dissimilar relationship between speed and acceleration, whereby, speed is dominant with minimal acceleration for flare-CMEs and eruptive-filament-CMEs have average speeds with maximum accelerations. Additional study based on LASCO has extended to 6621 CMEs to observe the definite CMEs classifications by studying their dynamic properties (Nicewicz et al. 2016). According to the data of velocity and acceleration, they came out with four CME classes with each of them possessed varying properties kinematically and physically and they also emerged in different methods.

Throughout solar cycle 23 and 24, the number of CME events in solar cycle 24 is more frequent than solar cycle 23 and the flare flux and CME mass are linearly related (Compagnino, Romano & Zuccarello 2017). Moreover, the onset time of flares during the CMEs (preceding or following) was also one of the factors that led to different relationships connecting with all properties (Shaltout et al. 2019). For both groups, the following-CMEs and preceding-CMEs have velocities and angular widths constantly associated as their correlation coefficients approaching the same values. On the study of CME productivity, it is largely influenced by the flare peak flux and flare duration as figured out by Yashiro et al. (2005), CMEs were greatly produced when there were increments in peak flux and flare duration. This result is supported with another study in 2018 where they obtained a convincing relationship between CME productivity and peak flux; flare-CMEs have higher peak flux that flares without CMEs (Suryanarayana et al. 2018). Besides, there was no evidence showing the flare duration affecting the flares peak flux, yet the strong flares usually occur due to serial filaments destabilization which then the energy is discharged from the sun's surface. Nevertheless, the flare duration does have an effect on CME mean angular width – prolonged flares have higher tendency to prompt the production of wide CMEs (Mawad, Abdel-Sattar & Farid 2021). On the relation between the kinetic energy of CMEs and flares energy, a study found an adequate correlation between both parameters whereby, major flares with higher energy, especially X-flares, are dominant in flare-CME events (Youssef 2012). Besides, a study presented and discussed on the formation of long-lasting B9 flare which was associated with CME and a filament eruption (Chandra et al. 2018). They found that although the associated flare was as low as B9, the events that were formed during the flare were quite significant and one of them was a partial halo CME. It emerged with an angular width of 225°, travelling a speed of 740 km/s and accelerating at 3.3 m/s^{-2}. The formation of the partial halo CME was also related to the filament eruption that was recognized by the bright core inside of the cavity as well as type II burst that confirmed the existence of the shock. Even though there are not many studies analyzing on the CMEs that can be caused by different type of flare classes, the stated findings from Chandra et al. (2018) and Youssef (2012) clearly showed two significant discoveries related to high X-flare and low B-flare. Therefore, it is important to also include lower flare classes by which this study included class A and B to examine the properties of CME that occur with lower flares.

In conclusion, many studies have proved variety of relationships between flares and CMEs, either positive or negative, their correlations are still significant and important to be analyzed on. Most of the studies focused on the kinematic of CME which are velocity, acceleration and angular width that are seen to correlate with specific parameter of flares. Therefore, this study is aimed to investigate whether the class of flare (A, B, C, M and X) contributes to the strength of CMEs in terms of their kinematic properties.

Methods

This study is carried out to analyze the distribution pattern of kinematic properties of different groups of flare-CMEs by looking at their velocity, acceleration and angular width altogether. The data is limited from Dec. 2008 until Dec. 2013 which is the beginning phase of solar cycle 24. Firstly, all events are sorted out according to which class of flare presence along with the respective CME. The CMEs that occurred with A, B and C flare are categorized as low group flare-CME and CMEs with M and X flare are then classified as high group flare-CME. All data and event images are obtained from the catalogue of Large Angle and Spectrometric Coronagraph (LASCO) instrument on board the Solar and Heliospheric Observatory satellite (SOHO).

In classifying the expected classes of CME, visual inspection is conducted on each event to distinguish the flares type during the CME commencement. Visual inspection is conducted by observing the formation time of CME and flares simultaneously on SOHO LASCO Catalogue and SpaceWeatherLive database. To view the evolution and propagation of the CME on a specific time, it can be done by clicking on the date and it will be directed to the movie as shown in Figure 1 (still images captured from the movie).

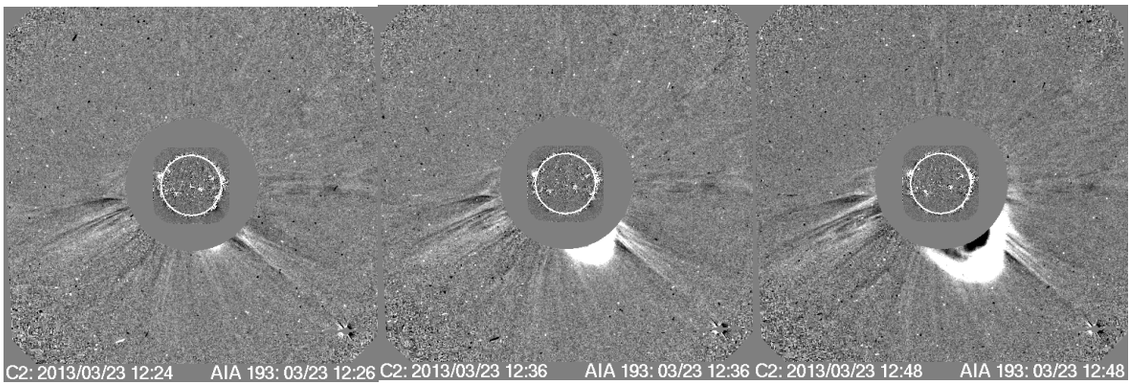

FIGURE 1. Still images of CME captured by LASCO on 23rd March 2013 (Brueckner et al. 1995)

TABLE 1. List of solar flares that occurred on 23rd March 2013 (NOAA 2022)

Region	Flare	Start	Maximum	End
1704	B5.4	01:49	01:58	02:02
1704	B6.8	02:04	02:09	02:14
1695	B5.5	02:29	02:40	03:28
1703	B6.8	12:15	12:22	12:27

As the information of CME have been obtained, SpaceWeatherLive database are then being analyzed afterwards to observe any flares erupted in the same time frame as the CME. Table 1 shows the list of solar flares recorded by NOAA SWPC throughout the day of the CME event which are later gathered and presented in SpaceWeatherLive database. This is one of the convenient ways to detect the associated flare with CME is by referring the list of solar flares that are recorded throughout the day as shown in Table 1. From the list, the solar flare that occurred together with CME can be recognized based on the start and end time of the flare. Based on the moving images recorded by SOHO LASCO, the partial halo CME took place within timeframe of 1224

UT until 1600 UT, which can be seen to be concurrent with B6.8 flare that is listed in Table 1.

Other than the flare list, observation on the x-ray flux in Figure 2 is also being referred to reconfirm the occurrence of B6.8 flare at the same time with the associate CME. The following graph plots the fluctuation of X-ray flux from 1200 UT until 1250 UT, whereby, a slight increment in the flux can be seen began at 1215 UT (as pointed in figure) and eased off a few minutes later. As this event is evidently taking place at the same instant with the CME, it can almost be concluded that both events are associated.

Afterwards, the position of the flare and CME also need to be observed to ensure both events emerged from the same region. Since the position of CME has been observed to be at the right below limb from the catalogue, the flare position can be confirmed from the SDO HMI image on SpaceWeatherLive. Figure 3 shows all regions that were presence on 23rd March 2013 and from the image, the AR 1703 is located at right below limb which is the exact place as CME. Therefore, it is concluded that the B5.6 flare and partial halo CME are coexisting and this event is classified under low group flare-CME because the associated flare is appeared to be low class flare.

Subsequently, all CMEs categorized according to their flare class as presented in Table 2. For the CMEs that are associated with low and high class flares, those events are not included in this study since this study is totally focusing on either low group flare-CME or high group flare-CME. The CMEs associated with both classes of flares might affect our data analyzation as the event would exist in both groups which could be the hidden factor to inaccurate results.

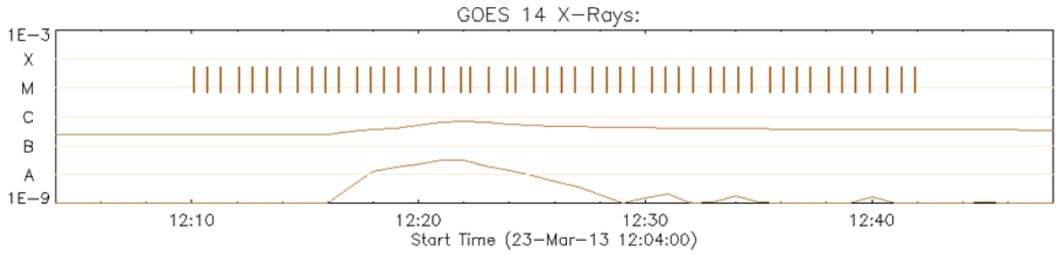

FIGURE 2. Plot of X-ray flux recorded by GOES-14 satellite Heliophysics Knowledgeable Event, 2022

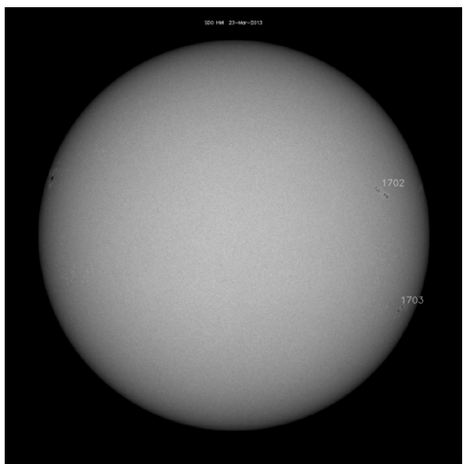

FIGURE 3. HMI Image of the Sun showing all regions presence on 23rd March 2013 (SDO 2022)

In order to achieve the correlations between each parameter, Pearson correlation coefficients are calculated for all variables. The Pearson correlation coefficient is the ideal measure of the strength of linear relationship between two variables (Kenton 2020), that is suitable to evaluate the dominance of a particular variable in CME events. Therefore, the Pearson correlation coefficient for each relationship between two parameters is calculated and presented in Seaborn heatmap to have a comprehensive figure of their relationships.

Results and Discussion

In this section, the distribution patterns of CME kinematic properties; velocity, acceleration and angular width for low group flare-CME and high group flare-CME along with their correlation coefficients are presented. The first stage in this study is to classify all CME events that took place in Dec. 2008 until Dec. 2013 into low group flare-CME or high group flare-CME. Over the period of five years, there were 3046 flare-CMEs reported, by which 2899 of them are accompanied by A, B and C flares and 147 CMEs were accompanied by M and X flares. Figure 4 shows the histogram displaying the velocity distribution of low group flare-CME and high group flare-CME.

Based on Figure 4 (left), the range of velocity of low group flare-CMEs is between 0-1000 km/s with more than half of the events are concentrated in the range of 0-500 km/s and less than 10 CMEs exceeded 2000 km/s. It is also noted that the major peak is around 250 km/s recorded by almost 500 CMEs and almost none of the CMEs travelled at the speed of 1500-2000 km/s. Meanwhile for high group flare-CME (Figure 4 right),

TABLE 2. CMEs classification according to group of flare and their respective energy

Classification	Low group flare-CME	High group flare-CME
Class of flare	A, B, C	M, X
Flare energy (W/m^2)	10^{-8} until 10^{-5}	10^{-5} until 10^{-3}

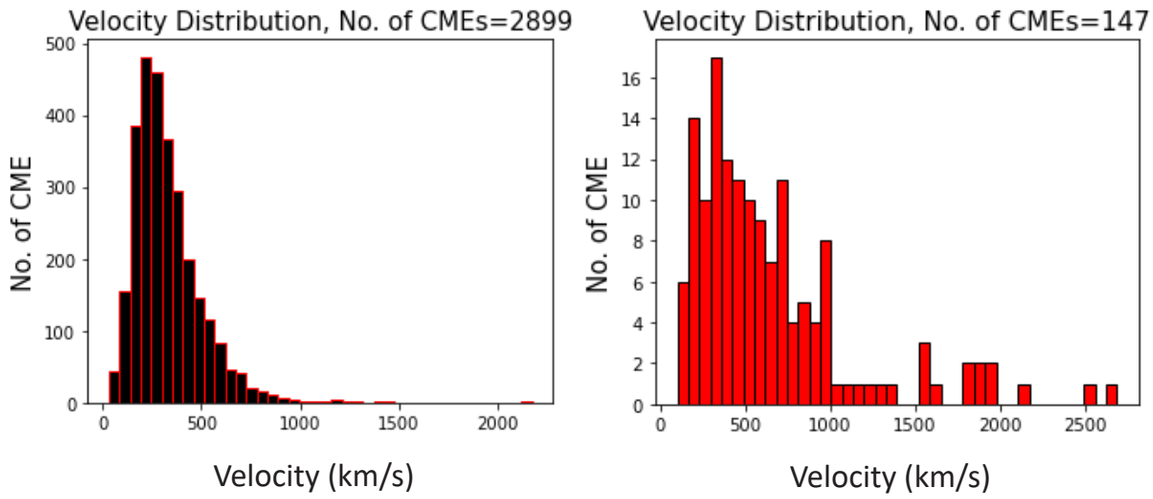

FIGURE 4. Histogram for the velocity for CMEs associated to low group flare-CME (left) and high group flare-CME (right)

the velocity range is more broader compared to low class flare-CME, whereby, out of 147 events, majority of them are accumulated in the range of 0-1000 km/s. While low group flare-CME barely has one event at velocity beyond 1500 km/s, high group flare-CME displays rather noticeable events at higher speeds, 1500 km/s and even over 2500 km/s. These results concur with the previous studies that showed CMEs that come along with major flares experience greater speeds (Andrews et al. 2001; Sheeley et al. 1999). Even though the total events for high group flare-CME is considerably low, the ratio of events with higher speeds to the total events is larger than low group flare-CME would have in their group, which implies that the domination of high velocity is more visible in high group flare-CME.

It has been proven that CMEs that are accompanied by high class flares tend to propagate at higher speeds. However, it is an interesting finding for CMEs that are associated with low class flares could exceed 500 km/s and above since those flares are sometimes recognized as background radiation. In order to obtain a convince analysis of a CME associated with low class flare, a further discussion on B6.3 flare that came along with a partial halo CME on 7th August 2013 is presented here to confirm their coexistence without any secondary events that might involve in the event. Figure 5 shows soft X-ray flux on 5th, 6th and 7th August 2013 by NOAA. It can be clearly seen that all flares recorded on the event day was B-class with the highest flare registered was B6.3 at 1902 UT.

Beside solar flares, CMEs can also be caused by coronal holes whereby high-speed solar wind takes place. On 7th August 2013, there was no presence of large coronal holes as shown in Figure 6, hence it is impossible for the partial halo CME to be influenced by high-speed solar wind event.

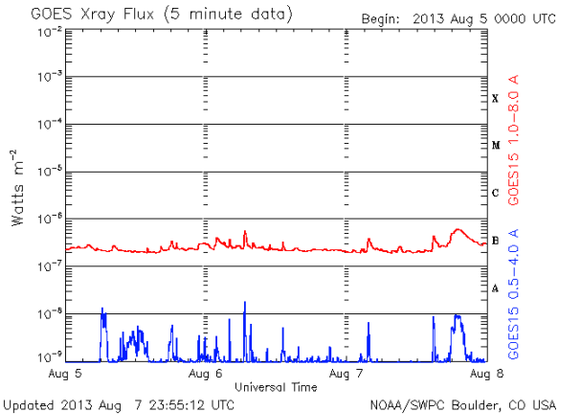

FIGURE 5. Soft X-ray flux on 5th, 6th and 7th August 2013 recorded by SWPC NOAA (NOAA; Möller)

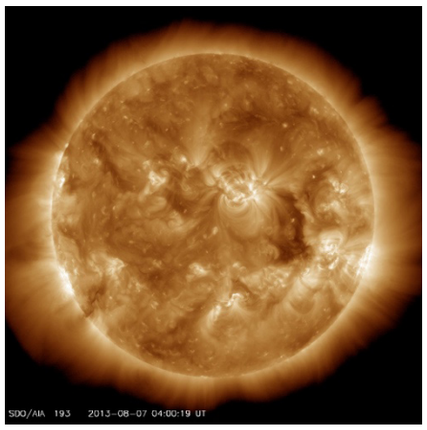

FIGURE 6. Image of coronal holes on 7th August 2013 in AIA filter (SDO 2022)

The B-flare erupted for over 3 hours by which it set off at 1713 UT, reached its peak at 1903 UT and eased off at 2031 UT. A closer look on the flare progression is presented in Figure 7 which displays at 1400 UT until 2300 UT. Based on the figure, the flare started its minimal climb at around 1700 UT, approached the maximum magnitude at 1900 UT and finished at 2030 UT.

Meanwhile, the partial halo CME started its eruption at 1824 UT and continued its development throughout the time frame of the B-flare event as presented in Figure 8. The concurrent of both events without the presence of coronal holes has convinced our analysis that B-flares, especially for long-lasting events, can also be the main driver for a CME despite their low energy.

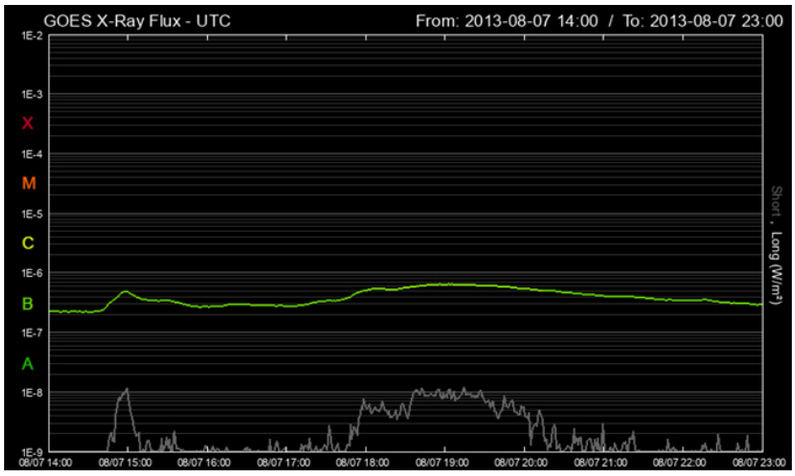

FIGURE 7. Plot of X-ray flux on 7th August 2013 (NOAA; Möller)

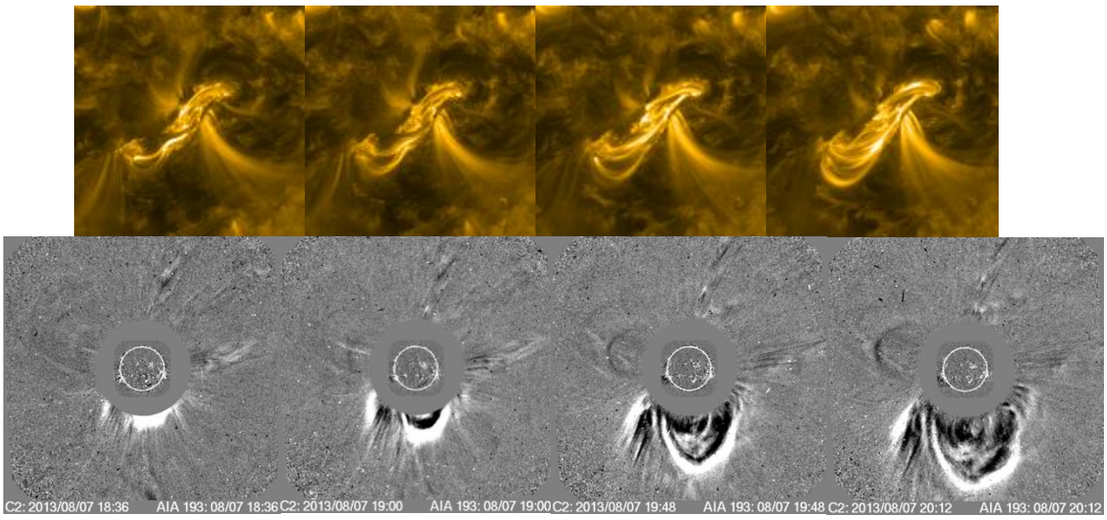

FIGURE 8. Emergence and evolution of partial halo CME and B6.3 flare on 7th August 2013 as viewed by LASCO C2 (Brueckner et al. 1995)

This result is supported by a previous study that found many flares associated with CMEs have a long-time span, suggesting a strong correlation between flare duration and CMEs (Kay et al. 2003). Additionally, Harrison (1995) once again justified that CMEs can be together with any class of flares in any duration, but long-lasting flares are most likely to have higher association with CMEs. Following the velocity analysis, acceleration of CME is also one of the important properties which is displayed in Figure 9. Figure 9 shows histogram for the acceleration of low group flare-CME and high group flare-CME.

The distribution pattern of acceleration for both classes are quite similar, whereby the peak can be seen close to 0 km/s with 1750 low group flare-CMEs and 40 events of high group flare-CME. This signifies that most of the flare-CMEs in the rising phase of SC24 moving at a constant speed during their propagations. Furthermore, the number of high group flare-CMEs going through deceleration are larger than low group flare-CMEs as the histogram (right) presents comparatively obvious growth at negative acceleration. These findings correspond to an earlier statistical study that have found that CMEs associated with M and X flares tend to approach constant speed - precisely, they manifest more decelerations (Moon et al. 2002). There is also several low group flare-CMEs that undergo deceleration but the ratio to the total events is slightly low, hence the are not significantly observed in the histogram.

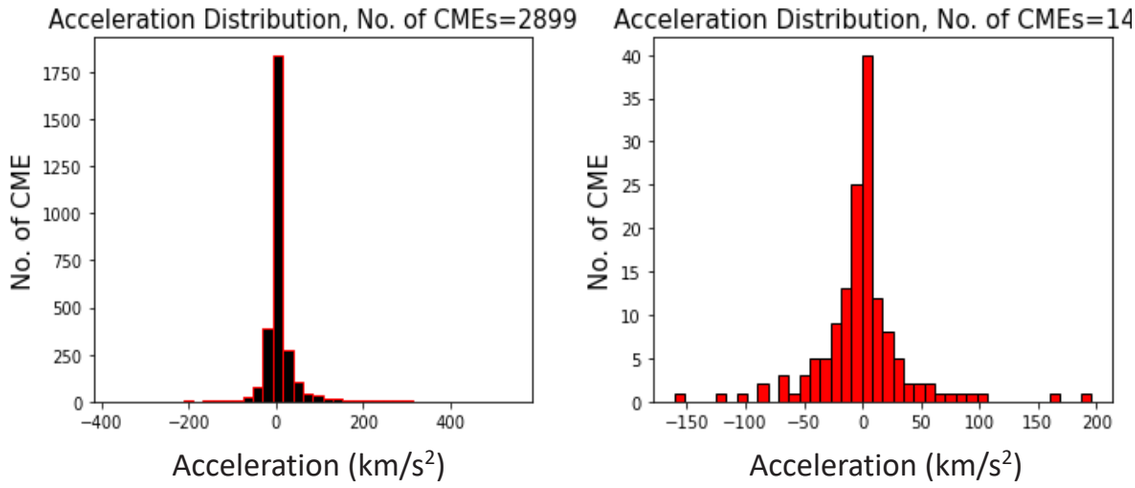

FIGURE 9. Histogram for the acceleration for CMEs associated to low group flare-CME (left) and high group flare-CME (right)

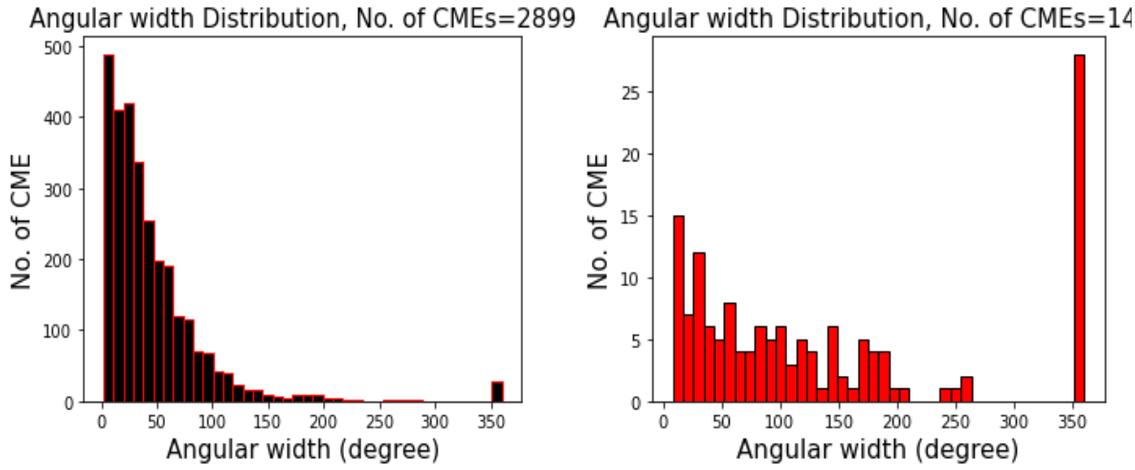

FIGURE 10. Histogram for the angular width for CMEs associated to low group flare-CME (left) and high group flare-CME (right)

The last kinematic properties to be discussed in this study is angular width. By referring to Figure 10, the distribution of angular width for both classes is thoroughly varying, by which low group flare-CME emerge not higher than type II halo (below 180°), while high group flare-CMEs frequently occur in a full halo (directly towards the Earth). The analyzed result demonstrates that high group flare-CMEs with angular width 360° occupy almost 20% proportion in the total events as highlighted in the right histogram. On the other side, the largest portion of low group flare-CME appear in the type I halo CME (90° and below) and very small percentage recorded with angular width of 360°. It is believed that A, B and C flares with energy of 10^{-8} - 10^{-5} W/m^2 are not sufficient to contribute additional energy to produce CMEs with wider angular width. The CMEs that go with M and X flares (10^{-5} until 10^{-3} W/m^2) have higher tendency to erupt in full halo as some of the energy from associated flares intensify the eruption. For a better comparison, the relationships between each property for both classes are presented in scatter plots as shown in Figure 11.

Figure 11 display scatter plots of kinematic properties of all CME events. Evidently, a great number of CMEs during the rising phase of SC24 were accompanied by low class flares as blue marks indicate saturated regions in all graphs. For the velocity-acceleration relationship in Figure 11(a), high group flare-CMEs are more scattered and outspread with broader range of velocity and as the velocity increases, the acceleration goes down approaching zero. A significant number of high group flare-CME also undergo deceleration with the

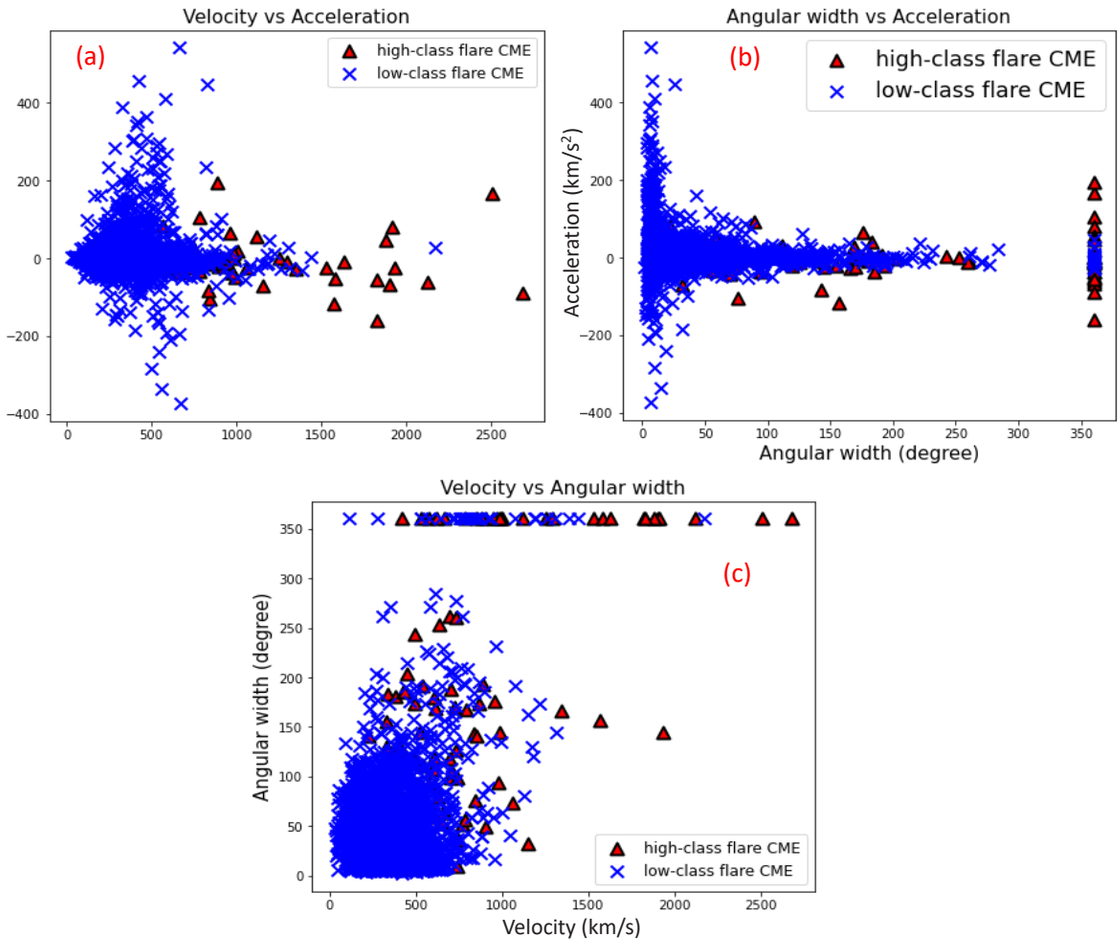

FIGURE 11. Scatter plot of (a) velocity vs. acceleration, (b) angular width vs. acceleration, (c) velocity vs. angular width

increment in velocity. Different situation presents for low group flare-CME, whereby the velocity does not run over the highest points obtained by high group flare-CME and there is an inclination of acceleration up to 500 km/s^2 at lower velocity.

The correlation between acceleration with angular width (Figure 11(b)) for both classes is quite identical as all events are located and spread out in the same pattern. It can be observed that high group flare-CMEs regularly generate full halo CME with fluctuating acceleration, while CMEs accompanied by minor flares tend to erupt in partial halo (≤ 180°) and their accelerations gradually drop as angular width increases. Following that, velocity and angular width also do not have much dissimilarity in their distributions as shown in Figure 11(c). All events are highly developed within 0-750 km/s with 0-150° width, despite associated class flare. The majority of high group flare-CMEs that emerge in 360° cover a wide range of velocity from 500 km/s and greater than 2500 km/s, which means there is not definite confines of how faster or slower full halo CMEs can travel. The same goes to low group flare-CME, whereby the CMEs that have 360° angular width have no absolute limit of velocity as they propagate at differing speed.

According to all results, almost all low group flare-CMEs that erupt for more than 30 min produce full halo CME although the associated flares energy is lower than M and X flares. Therefore, it is believed that low class flares that last longer than 30 min may supply the same amount of energy as M and X flares that can enhance the initiation of CME to create full halo. Figure 12 presents seaborn heatmap of Pearson correlation coefficient for both classes of CME.

Based on the Pearson correlation coefficient, velocity and angular width are the most correlated parameters for low group flare-CME with R=0.36, yet the value is quite low which means they are weakly correlated. The high group flare-CME also attain the same result and in fact, velocity and angular width are more eminently associated to each other with R value 0.67, about 31% higher than low group flare-CME. The weakest relationship is seen to be angular width and acceleration for high and low group with R= -0.059 and R= -0.096, respectively. A study investigating on slow and fast CMEs discovered that both groups of CME follow different power laws in width distribution depending on their speed, by which slow CMEs move

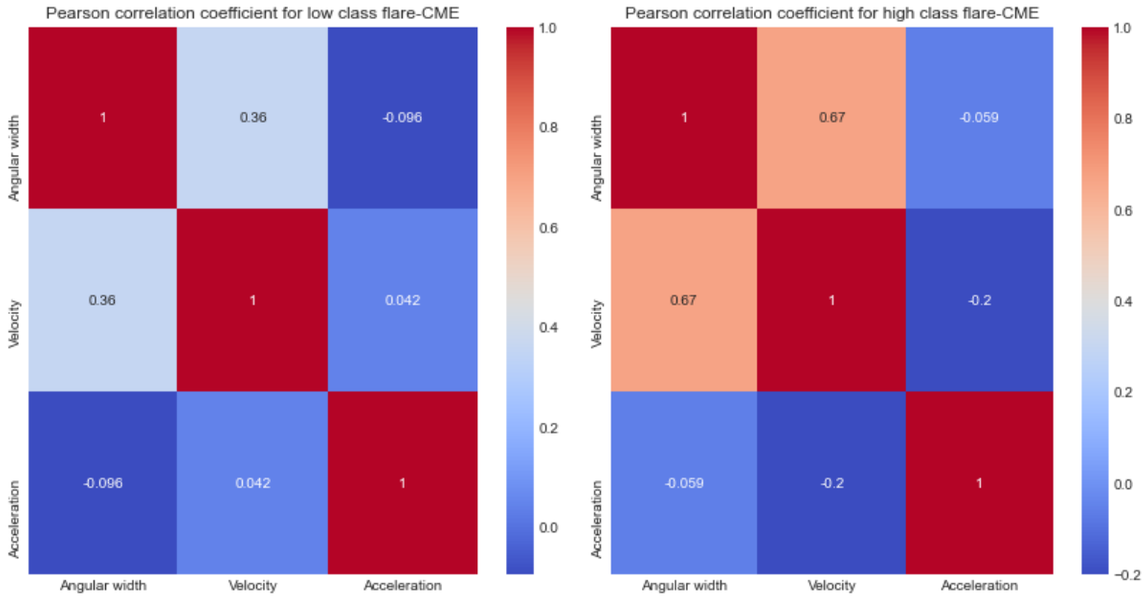

FIGURE 12. Values of Pearson correlation coefficient for low group flare-CME (left) and high group flare-CME (right)

towards steeper power law compared to fast CMEs (Pant et al. 2021). Moreover, observations on 23rd and 24th solar cycle found that maximum speed in 23rd cycle is 1556 km/s (wide CME) and 1103 km/s (intermediate CME) in 24th cycle, indicating a possible correlation between those parameters (Anna Lakshmi et al. 2011). As CMEs erupted, their propagation outwards from the Sun's limb travel through the background solar wind flow and it may crucially influence the CME expansion by means of velocity, acceleration or angular width. Therefore, it can be deduced that the most dominant CME parameters for flare-CME event are velocity and angular width and they are strongly influencing the development of flare-CME in the presence of major flares.

Conclusions

The overall flare-CMEs within Dec. 2008-Dec. 2013 recorded are 3046 events and they are categorized into low group flare-CME (2899 events) and high group flare-CME (147 events). For high group flare-CME, velocity-acceleration graph is outspread and they have wide-ranging velocity. When the velocity increases, acceleration undergoes declination towards zero and this occurs in large number of events. The velocity in low group flare-CME is not achieving higher values than high class and the acceleration begins to drop at 500 km/s and above. The high group flare-CME frequently take place in full halo (360°) with irregular pattern of acceleration and they usually arise within 500 km/s until above 2500 km/s. Meanwhile, angular width and acceleration are inversely correlated for low group flare-CME and majority of them do not exceed 180°. Besides, low class flares with any duration can also come along with CMEs despite their low energy and those that last long have higher possibility in associating with CMEs. For low and high groups, velocity and angular width are the most correlated parameters with R= 0.36 and R= 0.67, respectively, and the weakest correlation is found to be angular width and acceleration.

Acknowledgements

Special thanks go to SDO/AIA, NOAA, SWPC, LASCO, Helioviewer, Solar Monitor and Space Weather Live and E-CALLISTO websites for providing their data accessible to the public. Authors also give full appreciation to the reviewers and editors for the beneficial comments and suggestions. This work was partially supported by the Pembiayaan Yuran Penerbitan Artikel (PYPA) (RMC/UEP/3/1/2020).

References

Andrews, M.D. & Howard, R.A. 2001. A two-type classification of LASCO coronal mass ejection. *Space Science Reviews* 95: 147-163.

Anna Lakshmi, M., Umapathy, S., Prakash, O. & Vasanth, V. 2011. Studies on some properties of coronal mass ejections based on angular width. *Astrophysics and Space Science* 335(2): 373-378. DOI: 10.1007/s10509-011-0768-9

Brueckner, G.E., Howard, R.A., Koomen, M.J., Korendyke, C.M., Michels, D.J., Moses, J.D., Socker, D.G., Dere, K.P., Lamy, P.L., Llebaria, A., Bout, M.V., Schwenn, R., Simmett, G.M., Bedford, D.K. & Eyles, C.J. 1995. The Large Angle Spectroscopic Coronagraph (LASCO): Visible light coronal imaging and spectroscopy. *Solar Physics* 162(1-2): 357-402. DOI: 10.1007/BF00733434

Chandra, R., Chen, P.F., Fulara, A., Srivastava, A.K. & Uddin, W. 2018. A study of a long duration B9 flare-CME event and associated shock. *Advances in Space Research* 61(2): 705-714. DOI: 10.1016/j.asr.2017.10.034

Compagnino, A., Romano, P. & Zuccarello, F. 2017. A statistical study of CME properties and of the correlation between flares and CMEs over solar cycles 23 and 24. *Solar Physics* 292(1). DOI: 10.1007/s11207-016-1029-4

Gosling, J.T. 1994. Correction to 'The Solar Flare Myth'. *Journal of Geophysical Research* 99(A3): 4259. DOI: 10.1029/94JA00015

Harrison, R.A. 1995. The nature of solar flares associated with coronal mass ejection. *Astronomy and Astrophysics* 304: 585.

Heliophysics Knowledgeable Event. 2022.

Kay, H.R.M., Harra, L.K., Matthews, S.A., Culhane, J.L. & Green, L.M. 2003. The soft x-ray characteristics of solar flares, both with and without associated CMEs. *Astronomy & Astrophysics* 400(2): 779-784. DOI: 10.1051/0004-6361:20030095

Kenton, W. 2020. Pearson Coefficient.

MacQueen, R.M. & Fisher, R.R. 1983. The kinematics of solar inner coronal transients. *Solar Physics* 89: 89-102.

Mawad, R., Abdel-Sattar, W. & Farid, H.M. 2021. An association of CMEs with solar flares detected by Fermi γ-Ray burst monitor during solar cycle 24. *New Astronomy* 82. DOI: 10.1016/j.newast.2020.101450

Mittal, N. & Narain, U. 2010. Initiation of CMEs: A review. *Journal of Atmospheric and Solar-Terrestrial Physics* 72(9-10): 643-652. DOI: 10.1016/j.jastp.2010.03.011

Möller, A. 2022. GOES X-Ray Flux Archive.

Moon, Y.J., Choe, G.S., Wang, H., Park, Y.D., Gopalswamy, N., Yang, G. & Yashiro, S. 2002. A statistical study of two classes of coronal mass ejections. *The Astrophysical Journal* 581: 694.

Nicewicz, J. & Michalek, G. 2016. Classification of CMEs based on their dynamics. *Solar Physics* 291(5): 1417. DOI: 10.1007/s11207-016-0903-4

NOAA National Centers for Environmental Information. 2022.

Pant, V., Majumdar, S., Patel, R., Chauhan, A., Banerjee, D. & Gopalswamy, N. 2021. Investigating width distribution of slow and fast CMEs in solar cycles 23 and 24. *Frontiers in Astronomy and Space Sciences* 8. DOI: 10.3389/fspas.2021.634358

SDO Data. 2022.

Shaltout, A.M.K., Amin, E.A., Beheary, M.M. & Hamid, R.H. 2019. A statistical study of CME-associated flare during the Solar Cycle 24. *Advances in Space Research* 63(7): 2300-2311. DOI: 10.1016/j.asr.2018.12.022

Sheeley, N.R., Walters, J.H., Wang, Y.M. & Howard, R.A. 1999. Continuous tracking of coronal outflows: Two kinds of coronal mass ejections. *Journal of Geophysical Research: Space Physics* 104(A11): 24739-24767. DOI: 10.1029/1999ja900308

Suryanarayana, G.S. & Balakrishna, K.M. 2018. CME productivity associated with solar flare peak x-ray emission flux. *Advances in Space Research* 61(9): 2482-2489. DOI: 10.1016/j.asr.2018.02.008

Tousey, R. 1973. The solar corona. *Space Research Conference*. pp. 713-730.

Wolfson, R. & Dlamini, B. 1997. Cross-field currents: An energy source for coronal mass ejections? *The Astrophysical Journal*. p. 483.

Yashiro, S., Gopalswamy, N., Akiyama, S., Michalek, G. & Howard, R.A. 2005. Visibility of coronal mass ejections as a function of flare location and intensity. *Journal of Geophysical Research* 110(A12). DOI: 10.1029/2005JA011151

Youssef, M. 2012. On the relation between the CMEs and the solar flares. *NRIAG Journal of Astronomy and Geophysics* 1(2): 172-178. DOI: 10.1016/j.nrjag.2012.12.014

*Corresponding author; email: zetysh@uitm.edu.my